ELSEVIER

Fire Safety Journal 33 (1999) 21–34

FIRE SAFETY JOURNAL

www.elsevier.com/locate/firesaf

Numerical and experimental gravity currents related to backdrafts

C.M. Fleischmann[a,*], K.B. McGrattan[b]

[a]Department of Civil Engineering, University of Canterbury, Christchurch, New Zealand
[b]Building and Fire Research Laboratory, National Institute of Standards and Technology, Gaithersburg, MD 20899, USA

Received 26 June 1998; received in revised form 23 September 1998; accepted 17 November 1998

Abstract

In order to clarify the mixing that occurs in a gravity current which precedes a backdraft, a two-dimensional simulation, a series of salt water experiments, and backdraft experiments were performed. A compartment in a ratio width/height/length of 1/1/2 is used in the experiments and computations. Two different openings were used in the salt water experiments and numerical computations: a fully open end wall and a $h_1/3$ horizontal slot centred in an end wall, where h_1 is the compartment height. For the backdraft experiments only the $h_1/3$ horizontal slot was used. The visual observations from the salt water experiments compare well with the numerical simulation. Both show a small mixed region at the gravity current shear interface for the fully open wall and mixing throughout the entire current for the $h_1/3$ horizontal slot. Quantitative comparisons are made in terms of the normalised density differences, $\beta = (\rho_0 - \rho_1)/\rho_1$, where ρ_0 is the higher density and ρ_1 is the lower density. The transit time results, i.e., time between opening the compartment and the time the gravity current reaches the wall opposite the opening, for the computations compared favourably with the transit times from the salt water experiments, over the range $0.003 < \beta < 0.100$. Velocity measurements from the opening of the backdraft compartment, prior to ignition, also are favourable with the numerical simulation. © 1999 Elsevier Science Ltd. All rights reserved.

Nomenclature

$C(\mathrm{Re})$	empirical correction factor for Eq. (6)
c	salt water mass fraction

* Corresponding author. Tel.: 0064-3-364-2399; fax: 0064-3-364-2758.
E-mail address: fleisccm@cad.canterbury.ac.nz (C.M. Fleischmann)

PII: S0379-7112(98)00046-0

D	diffusion coefficient
$\mathbf{g}$	acceleration of gravity
h_1	height of the compartment
L	length of the comparment
p	pressure
Re	Reynolds number
Sc	Schmidt number
t^*	characteristic time
t	time
U	characteristic velocity, $=\sqrt{\beta g h_1}$
$\mathbf{u}$	velocity vector
v	velocity at the bidirectional probe
β	density difference ratio, $\beta = (\rho_0 - \rho_1)/\rho_1$
ν	kinematic viscosity
ρ	total local density of the mixture
ρ_0	ambient density outside of the compartment
ρ_1	density inside the compartment
ρ_v	density at the bidirectional probe calculated from the temperature

1. Introduction

When a fire occurs in a closed compartment where the only ventilation is due to leakage, the fire can become limited by the available oxygen and produce large amounts of unburned fuel. If the leakage rate is low enough the fire may enter a smoldering stage. Temperatures within the compartment will be low compared with flashover temperatures but significantly higher than the ambient. The higher temperatures decrease the average compartment density below the ambient density. When the compartment is opened, a density-driven flow, referred to as a gravity current, enters the compartment. The dense ambient air pours through the opening mixing with the hot compartment gas as the current travels across the floor. If the fuel concentrations are high enough and the gravity current comes in contact with an ignition source, a backdraft will rip through the compartment injuring any unsuspecting firefighters trapped in the rapidly advancing flame [1]. A better understanding of gravity currents which enter the compartment is necessary to improve our knowledge of the backdraft phenomena.

A large body of research is available on the subject of gravity currents [2–4]. Much of this research involves laboratory-scale salt water models. Typically, salt water models do not provide complete answers to gravity current questions. Some important detail is lost when a salt water model is used including the large vortical structure typically seen in shear flow problems.

In this paper, a two-dimensional numerical simulation is used to analyse the gravity current as it enters a fire compartment. The results of the two-dimensional computations provide valuable insight into the detailed structure of the gravity current. The results of the numerical simulation are compared with the results from two different experiments. In the first set of experiments, a salt water model with two fluids of different density is used to visualise the flow into the compartment [5]. The second set of experiments uses a half domestic scale, 1.2 m × 1.2 m × 2.4 m, compartment to produce backdrafts in the laboratory. Data collected (prior to ignition) in the backdraft experiments are compared with both the salt water and numerical results.

2. Numerical modeling

Consider the buoyancy-driven flow induced by the interaction of salt water and fresh water initially separated by a vertical interface. The equations of motion for this incompressible, isothermal mixture are:

$$\mathbf{div}(\mathbf{u}) = 0, \tag{1}$$

$$\partial(\rho c)/\partial t + \mathbf{div}(\rho c\mathbf{u}) = \mathbf{div}(\rho D \nabla c), \tag{2}$$

$$\rho(\partial \mathbf{u}/\partial t + \mathbf{u}\cdot \nabla\mathbf{u}) + \nabla p - \rho\mathbf{g} = \rho\nu\nabla^2\mathbf{u}, \tag{3}$$

where c is the salt water mass fraction (defined as the ratio of the mass of salt water to the total mass of fluid in a given volume element) $\mathbf{u}$, is the velocity vector, p is the pressure, $\mathbf{g}$ is the acceleration of gravity, ν is the kinematic viscosity, and D is the diffusion coefficient. The latter two quantities will be assumed to be constant. The density of the mixture may be expressed as and $\rho = \rho_1(1 + \beta\tilde{\rho})$, where $\beta = (\rho_0 - \rho_1)/\rho_1$; and ρ_1 and ρ_0 are the densities of the fresh and salt water, respectively. In terms of β and $\tilde{\rho}$, the mass fraction c may be written as

$$c = \tilde{\rho}(1 + \beta)/(1 + \beta\tilde{\rho}). \tag{4}$$

We are interested here in the motion of the fluid mixture in a two-dimensional polygonal configuration, consisting of a small chamber initially filled with a fresh water, separated from the salt water outside by a vertical interface. Eqs. (1)–(3) are solved numerically in non-dimensional form using finite differences. The Reynolds and Schmidt numbers that result from the scaling are given by $\mathrm{Re} = Uh_1/\nu$ and $\mathrm{Sc} = \nu/D$ where U is a characteristic velocity related to the Froude scaling $U = \sqrt{\beta g h_1}$, and h_1 is the height of the enclosure.

An alternating direction implicit numerical scheme was used to solve the above equations. Details of the numerical method may be found in Ref. [6]. For the comparisons with the salt water and backdraft experiments shown here, computations were performed on the IBM RISC System/6000 Model 550 at NIST. A typical computation required between 20 and 80 megabytes of memory and 5 to 25 hr of CPU time. The resolution of the computational grid determines the maximum Reynolds number for a given run. Roughly, this maximum value scales as K^2, where K is the number of grid cells in the direction of the length scale h_1. The largest Reynolds number reported here is 50,000, and this simulation required a grid of dimension 1024 × 256.

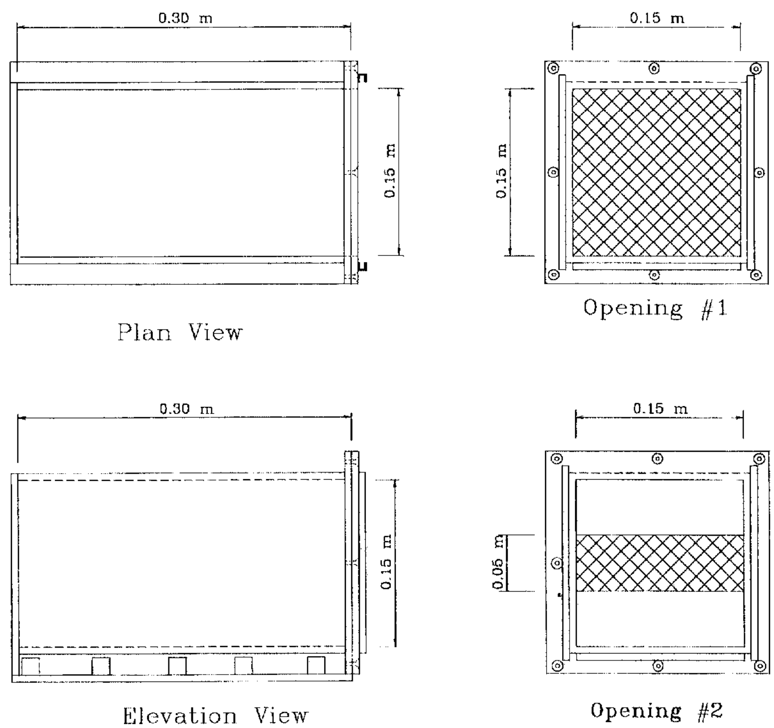

Fig. 1. Sketch of salt water chamber showing the elevation and plan views as well as opening geometries.

3. Salt water experimental apparatus and procedures

Salt water experiments were conducted by placing an acrylic chamber within a larger glass tank. The chamber was constructed from 6 mm thick acrylic with interior dimensions of 0.15 m wide, 0.30 m long and 0.15 m high. Fig. 1 shows the plan and elevation views along with the opening geometries for the chamber. Two two-dimensional opening geometries were used, as seen in Fig. 1, the cross hatched area indicates the opening. The end opening was covered with a vertical sliding partition that was removed to start the experiment. The large tank, 0.3 m wide, 0.6 m long, and 0.45 m deep, contained a dense water and salt solution ranging in density from 1.003 to 1.101 kg/m^3.

The solution in the chamber was regular tap water with a pH of 6.8 and a density of 1000 kg/m^3. A small amount of phenolphthalein ($>2\times10^{-4}$ M) was added to the chamber. Phenolphthalein, a common pH indicator, was used to visualize the gravity current. When phenolphthalein mixes with a base, in this case sodium hydroxide crystals were added to the large tank to raise the pH to 11.7, the product of the reaction is red. This reaction is believed to be diffusion limited. The red product is strongly visible even in dilute concentrations. Turbulence is unaffected by the reaction since there is little surface tension, buoyancy, or heat release produced by the reaction. Unlike passive scalar techniques, such as dye, this chemical reaction is a much better indicator of the mixing within the gravity current. A formal discussion of this technique is given by Breidenthal [7].

Once the two solutions were prepared, specific gravity, temperature, and pH were recorded. The chamber was then lowered into the tank and the partition on the chamber was removed within 120 s to avoid leakage effects. Within 0.1 s the partition was completely clear of the opening. The gravity current was recorded using a 8 mm video camcorder at 30 frames/s. A more complete discussion of the apparatus and procedures used in the salt water modelling can be found in Ref. [8].

4. Backdraft experimental apparatus

A second series of experiments was conducted using a half domestic scale compartment filled with hot gases from a methane fueled gas burner. Fig. 2 is a sketch of the compartment. In one of the short walls, a 0.4 m high, 1.1 m wide opening was centred vertically. A 0.3 m square gas burner, with a horizontal surface 0.3 m off the floor and centred horizontally along the wall opposite the opening, provided the initial fire

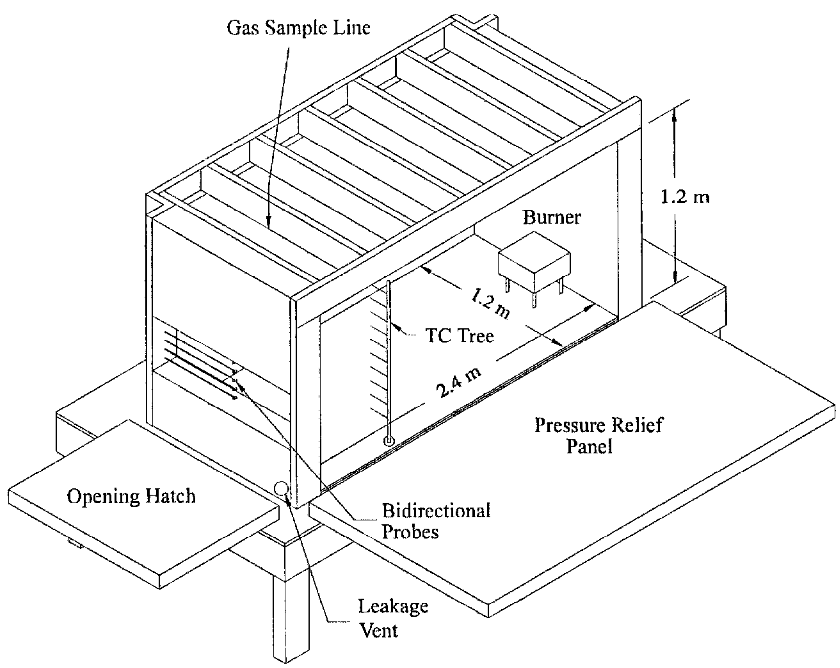

Fig. 2. Sketch of the half domestic scale backdraft compartment showing important features of the apparatus.

within the compartment. Gas flow to the burner varied from 70 to 200 kW of technical (98% pure) methane.

A computer-controlled hatch, hinged at the bottom, covered the slot until a predetermined opening time was reached. In the slot, six bidirectional probes were installed in a vertical rake. The probes were 17 mm in diameter and designed in accordance with the guidelines given by McCaffrey and Heskestad [9]. The probes were evenly spaced, 65 mm apart centred horizontally in the opening and numbered sequentially from the top down. The top (# 1) and bottom (# 6) probes were 43 mm from the soffit and sill, respectively. The bidirectional probes were oriented horizontally to avoid incorrect readings due to buoyancy effects. The pressure differential was measured using a differential pressure transducer which had a calibrated range of $\pm$ 25 Pa. The response time of the transducer was 30 μs. Readings were recorded approximately 50 times a second and a 11 point smoothing routine was applied to the data. Bare bead thermocouples made from 0.5 mm type K wire, with an average bead diameter of 1.1 mm were placed at each probe to measure the temperature as required for density calculations. No correction was applied to the thermocouple data. Aspirated thermocouples placed in close proximity to the probes indicated that a radiation correction was unnecessary.

In each experiment, the gas burner was ignited in the closed room. The fire burned until the burner could no longer support combustion due to a lack of oxygen. The burner was then left on to allow unburned fuel to accumulate. At a predetermined time, the burner was turned off and 5 s later the hatch was opened to allow the gravity current to enter the compartment. The response time of these thermocouples was adequate for the gravity current. The backdraft was initiated by an electric arc located 0.45 m above the floor and centred over the top of the burner. Additional details can be found in the Ref. [8].

5. Qualitative results

Fig. 3a shows the density field from the numerical simulation for the fully open condition. The black color represents the compartment fluid and the lightest grey colour is the ambient fluid. Looking at Fig. 3a the gravity current can be divided into two regions: region 1 is purely ambient, cold fluid which is moving toward the head of the gravity current and region 2 is the mixed layer along the shear interface which consists of hot, fuel rich, compartment fluid rolled up within large coherent structure of cold, oxygen-rich ambient fluid.

Fig. 3b is a photograph from the salt water experiments for the fully open case at approximately the same location as Fig. 3a. The photograph closely resembles the numerical simulation results. Region 1 is the clear salt water which indicates that no phenolphthalein has reached that portion of the gravity current. The mixed layer, region 2, is the grey (red) area along the shear interface. The large vortical structure seen in the numerical simulation is not visible here because the photograph of the salt water experiment is an integral along a line of sight across the entire width of the chamber and the details of the structure are lost. Experiments by Simpson [10] show

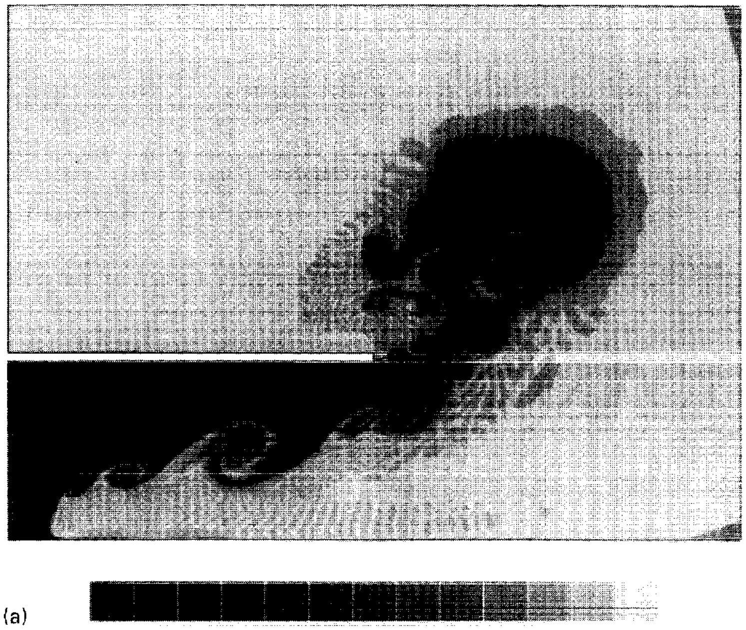

(a)

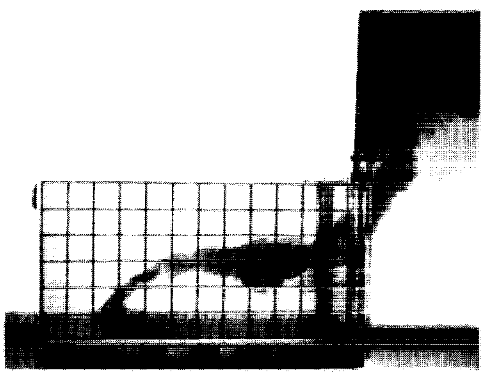

(b)

Fig. 3. (a) Density profile for the full opening case. Shown here after 4.0 non-dimensional time units. Reynolds number is 20,000. (b) Photograph of the gravity current approximately 3 1/4 into the compartment for the fully open condition. The grid shown on the model is 25 mm squares, $L = 0.018$.

similar large vortices when vertical slit lighting and fluorescent dye are used to illuminate a more-two dimensional image of a steady-state gravity current.

Fig. 4a shows the computed density profile for the $h_1/3$ centred slot opening condition. The structure of the gravity current is significantly different from the full opening case. The current cannot be divided up into two distinct regions as in fully open case. Large vortices make up the entire gravity current for the slot opening. The coherent

(a)

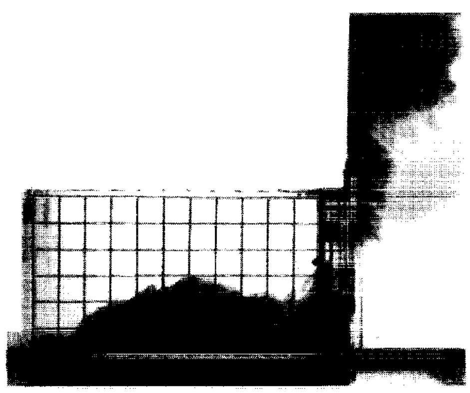

(b)

Fig. 4. (a) Density profile for the $h_1/3$ centred slot opening case. Shown here after 6.8 non-dimensional time units. Reynolds number is 20,000. (b) Photograph of the gravity current approximately 3 $L/4$ into the compartment for $h_1/3$ centred slot opening, $\beta = 0.024$.

structure making up the gravity current indicates that large-scale mixing is occurring. The increased mixing is caused by the $h_1/3$ centred slot opening acting as a rearward facing step which is a well-known source of large vortical structures.

Fig. 4b is a photograph of the salt water experiment with the $h_1/3$ centred slot opening showing the gravity current in approximately the same location as Fig. 4a.

The large-scale mixing predicted by the computations is seen as the dark grey colour throughout the gravity current. From these results, it can be seen that the simple two region model used for steady-state gravity currents works for the full opening but cannot be applied to the slot opening condition.

6. Quantitative results

To quantitatively compare the numerical simulation with the experiments, the gravity current transit time is used. The transit time is the time required for the leading edge of the gravity current to reach the wall opposite the opening. For the numerical simulation the transit time was determined when the density at the rear wall changed by 10%. In the salt water experiments, the transit time was taken from video recordings of the gravity current. The results are presented in non-dimensional form where

$$\frac{t}{t^*} = \frac{L}{U} = \frac{L}{\sqrt{\beta g h_1}}. \tag{5}$$

Fig. 5 shows the non-dimensional transit times versus relative density difference, β, for the full and slot opening conditions, respectively. There is excellent agreement between the salt water model and the numerical simulation for the fully open condition. For the $h_1/3$ centred slot opening, the agreement is not as favourable as the fully

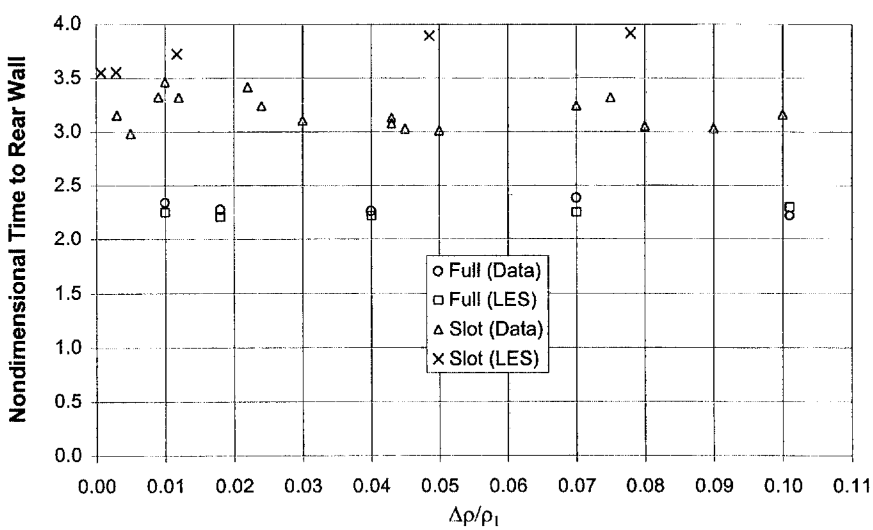

Fig. 5. Plot of the non-dimensional time for the gravity current to reach the rear of the saltwater compartment versus density difference, β. LES model fully open case (□), saltwater modelling results fully open case (○), LES modelling slot opening case (×), saltwater modelling results slot opening case (△).

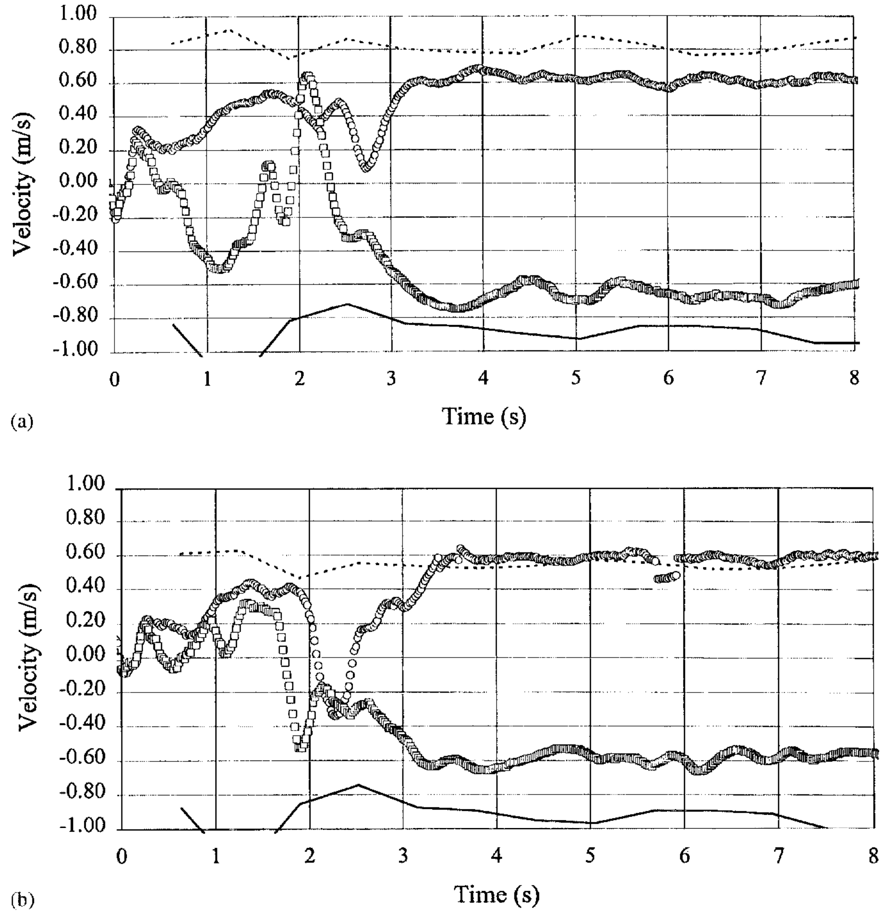

Fig. 6. (a) Plot showing the velocity history for the probe #1 (○) and #6 (□) in the opening of the backdraft compartment compared with the numerical simulation results shown as, probe #1 (- - - -) and probe #6 (——). (b) Plot showing the velocity history for the probe 2 (○) and 5 (□) in the opening of the backdraft compartment compared with the numerical simulation results shown as, probe 2 (- - - -) and probe 5 (——).

open case. Computed values are consistently longer than the values measured in the salt water experiments.

From the backdraft compartment experiments, a comparison between the numerical simulation and the bidirectional probes located in the opening is made. The probe velocity is calculated using the relationship suggested by McCaffrey and Heskestad [9]:

$$v = C(\mathrm{Re})\sqrt{\frac{2\Delta p}{\rho}}, \tag{6}$$

where v is the velocity at the probe, Δp is the pressure difference measured across the probe, ρ is the local density, and $C(\mathrm{Re})$ is an empirical calibration constant which is a function of the Reynolds number. Typically, $C(\mathrm{Re})$ is taken as a constant of 0.926 which gives a maximum error of 7% for $\mathrm{Re} > 520$. In this case, the Re was smaller, $\mathrm{Re} \sim 300$, so the following calibration constant was required:

$$\frac{1}{C(\mathrm{Re})} = 1.533 - 1.366 \times 10^{-3}\,\mathrm{Re} + 1.688 \times 10^{-6}\,\mathrm{Re}^2 - 9.706 \times 10^{-10}\,\mathrm{Re}^3 + 2.55 \times 10^{-13}\,\mathrm{Re}^4 - 2.484 \times 10^{-17}\,\mathrm{Re}^5. \tag{7}$$

Eqs. (6) and (7) are applicable for $40 < \mathrm{Re} < 3800$. For $\mathrm{Re} < 40$, the velocity is less than 0.07 m/s and is considered negligible.

Fig. 6a and b compare the velocity history for probes 1, 2, 5 and 6 with the numerical simulation for $\beta = 0.52$. Negative velocities indicate flows into the compartment. The hatch was released at 0 s. At approximately 1.5 s the opening hatch strikes the table and causes excessive noise in the data. From 0 to 4 s the flow in the opening is developing. After approximately 4 s the flow can be assumed to be quasisteady. At 4 s the total mass flow into the chamber is 0.28 kg and the gravity current is approximately $3\,L/4$ into the compartment as shown in Fig. 4. Once ignition occurs, the comparison between the experiments and calculations ends as the numerical simulation cannot model the ignition or subsequent backdraft. If ignition does not occur, the flow will slowly diminish to zero as the compartment cools. The flow into and out of the compartment which continues long after the initial gravity current has subsided is the result of the thermal energy stored in the boundaries heating the incoming air and driving the flow. In one experiment where the ignition was delayed for 600 s, the velocity dropped to ~ 0.2 m/s.

Fig. 7 shows the vertical velocity profile in the opening at different times. The lines show the numerical simulation and the symbols are the experimental data. At 4 s the

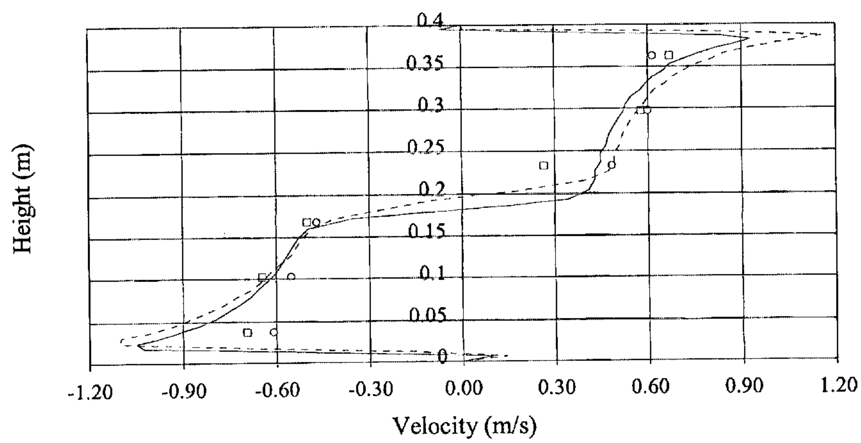

Fig. 7. Plot of the velocity profiles in the opening of the backdraft compartment shown at 4 and 8 s after opening. Numerical simulation results are shown as lines and the experimental data are shown as symbols. (4 s □ - - - -) (8 s ○ ——).

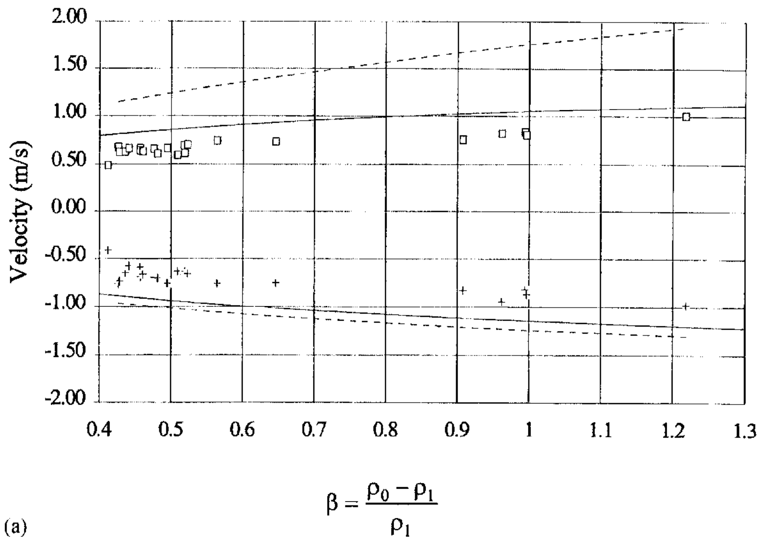

(a)

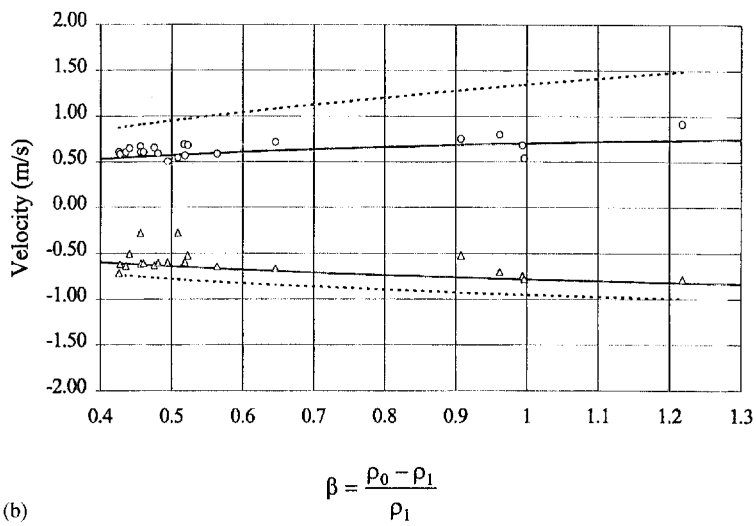

(b)

Fig. 8. (a) Plot of the quasisteady velocity in the opening of the backdraft compartment versus density difference ratio, β. The experimental data are indicated as symbols, the numerical simulation is shown as solid lines, and the potential flow result is shown as a dashed line. (probe 1 □) (probe 6 +). (b) Plot of the quasisteady velocity in the opening of the backdraft compartment versus density difference ratio, β. The experimental data are indicated as symbols, the numerical simulation is shown as solid lines, and the potential flow result is shown as a dashed line. (probe 2 ○) (probe 5 △).

data indicate that the flow has developed into the expected in/out profile and show excellent agreement with the numerical simulation. The velocity profile shows little change prior to 8 s when the spark is activated and ignition occurs.

Fig. 8a and b are plots of quasisteady velocity in the opening versus β. Data are shown as discrete points, numerical simulation results are the solid lines, and potential flow results are the dashed lines [11]. There is good agreement between the experimental opening velocities and the numerical results, with the numerical result being consistently higher than the data. The potential flow result is almost a factor of 2 greater than the measured result which indicates that assumption, as expected, oversimplifies the problem. The numerical simulation is much closer to the measured values. The differences between experiments and computation are likely to be due to 3D effects not included in the simulation and the large errors which can be expected in the measurements at this low velocity. For velocities of O(1 m/s), the experimental error is as high as $\pm 40\%$.

7. Conclusions

The two-dimensional numerical simulation presented here shows good agreement when compared with the compartment gravity current for the fully open condition. The two-dimensional computational density profile shows that the main body of the current is made up ambient fluid while a mixed layer made up of large vortical structures exists along the shear interface between the two fluids. Such structure is also observed in the salt water experiments although the individual vortices are not resolved due to the limitations of the flow visualisation techniques. Results of other researchers [10] indicate that large vortices do occur behind the head of a steadily propagating gravity current which are similar in appearance to the transient compartment gravity current results shown here.

For the slot opening, the results of the two-dimensional simulation compare favourably with the experimental results. The computed density profile shows that the structure of the gravity current for the $h_1/3$ centred slot opening is significantly different from the fully open condition. For the slot opening, the entire gravity current is filled with a complex structure of large-scale vortices which translates into large-scale mixing. This large-scale mixing for the $h_1/3$ centred slot opening results from the rearward facing step, formed by the lower edge of the slot.

Transit times predicted by the numerical simulation compare well with the salt water experiments although the computed times are slightly longer for the slot opening. Numerical velocity profile predictions in the opening compared well with backdraft experiment results, falling well within the experimental error bounds.

Future work should focus on different compartment aspect ratios, smaller openings, and openings at the floor level. There have been limited studies involving radially spreading gravity currents, however, additional work is required [5,12]. Improved flow visualisation techniques including a laser sheet to obtain a two-dimensional image of the gravity current are recommended. Time-dependent concentrations and velocities should be measured within the gravity current for comparison with computational results.

Acknowledgements

National Institute of Standards and Technology, Building Fire Research Laboratory, Grant No. 6ONANB1D1168 partially supported this work. Discussions with P.J. Pagni, H.R. Baum, R.G. Rehm, and R.B. Williamson contributed significantly to this paper. Assistance from J. Fleischmann and A. Revenaugh with the experiments and photography is appreciated. Editorial assistance of C. Grant and C. Caldwell is warmly acknowledged.

References

[1] Fleischmann CM, Pagni PJ, Williamson RB. Exploratory backdraft experiments. Fire Technol 1993;29:298–316.
[2] Benjamin TB. Gravity currents and related phenomenon. J Fluid Mech 1968;31:209–248.
[3] Simpson JE. Gravity currents in the laboratory, atmosphere, and ocean. Ann Rev Fluid Mech 1972;14:213–234.
[4] Steckler KD. Fire induced flows in corridors — a review of efforts to model key features. NISTIR-89-4050, National Institute of Standards and Technology, Gaithersburg, MD, 1987.
[5] Fleischmann CM, Pagni PJ, Williamson RB. Salt water modeling of fire compartment gravity currents. 4th Int Symp on Fire Safety Science, International Association of Fire Safety Scientist, 1994:253–264.
[6] McGrattan KB, Rehm RG, Tang HC, Baum HR. A boussinesq algorithm for buoyant convection in polygonal domains NISTIR 4831. National Institute of Standards and Technology, Gaithersburg, MD, 1992.
[7] Breidenthal R. Structure in turbulent mixing layers and wakes using a chemical reaction. J Fluid Mech 1981;109:1–24.
[8] Fleischmann CM. Backdraft phenomena. NIST-GCR-94-646, National Institute of Standards and Technology, Gaithersburg, MD, 1994.
[9] McCaffrey BJ, Heskestad G. A robust bidirectional low-velocity probe for flame and fire application. Combust Flame 1976;26:125–127.
[10] Simpson JE. Effects of the lower boundary on the head of a gravity current. J Fluid Mech 1972;53:759–768.
[11] Babrauskas V, Williamson RB. Post flashover compartment fires: basis of a theoretical model. Fire Mater 1978;2(2).
[12] Lane-Serff GF. 1989 Laboratory models of transient, buoyancy-driven flow. Ventilation '88, Conference proceedings ISBN 0-008-036148-X.